

NANOCOMPOSITE APPLICATION FOR SELENIUM REMOVAL – PARAMETRIC STUDIES AND KINETIC MODELING

N. RAJAMOHAN^{1,*}, M. RAJASIMMAN²,
FATMA AL QASMI¹, ELDON RENE³

¹Chemical Engineering Section, Sohar University, Sohar, Sultanate of Oman
²Environmental Engineering Laboratory, Department of Chemical Engineering,
Annamalai University, Annamalai Nagar, India
³UNESCO-IHE Institute for Water Education, Delft, Netherlands
*Corresponding Author: rnatarajan@soharuni.edu.om

Abstract

Nano composite material was synthesized using calcium hydroxy apatite and *Phoenix Dactylifera* tree powder using wet chemical precipitation method and characterized using scanning electron microscopy and Fourier transform infrared spectroscopy. The influence of operating parameters namely initial pH (3 -11), selenium concentration (50 -200 mg L⁻¹), nanocomposite dose (0.5 - 6.0 g L⁻¹), presence of competitor chloride ion (0 -10 g L⁻¹) and agitation speed (0 – 600 rpm) on the metal uptake was studied. A correlation relating nano composite dose and selenium uptake was proposed as selenium uptake = 202.3 (e-0.259* nanocomposite dose) he maximum uptake capacity of the nanocomposite was found to be 57.27 mg g⁻¹ under optimal environmental conditions with an initial selenium concentration of 100 mg L⁻¹. Monolayer sorption mechanism, proposed by Langmuir isotherm, was found to apply for this process and the isotherm constants were determined. Modified Ritchie second order and pseudo second order models were fitted to the experimental data and pseudo second order model correlated well with rate constant of 1.5 x 10⁻³ g mg⁻¹ min⁻¹ and maximum uptake capacity of 70.92 mg g⁻¹ at 32 °C with 100 mg L⁻¹ initial metal concentration. Ritchie model rate constant was evaluated as 1.41×10⁻² min⁻¹ under similar process conditions.

Keywords: Efficiency, kinetic model, nanocomposite, selenium.

1. Introduction

Natural ecosystem balance and composition is manipulated unconvincingly through uncontrolled discharge of metal pollutants in the environment by anthropogenic sources. Presence of metals poses a higher degree of pollution risk

Nomenclatures

C_e	Concentration of Selenium at equilibrium, mg L ⁻¹
C_o	Initial concentration of the Selenium, mg L ⁻¹
K_F	Freundlich constant, mg g ⁻¹
K_L	Langmuir constant, L mg ⁻¹
k_2	Equilibrium rate constant for pseudo-second order adsorption, g mg ⁻¹ min ⁻¹
k_R	Equilibrium rate constant for modified Ritchie model, min ⁻¹
q_e	Amount of Selenium adsorbed on the adsorbent at equilibrium, mg g ⁻¹
q_{max}	Maximum adsorption capacity, mg g ⁻¹
q_t	Amount of Selenium adsorbed at time, t, mg g ⁻¹
V	Volume of the solution, L
w	Nanocomposite dose, g L ⁻¹
$1/n$	Adsorption intensity

Abbreviations

ABNC	Agro Based Nano Composite
FTIR	Fourier Transform Infra Red
SEM	Scanning Electron Microscope

due to their tendency to resist biodegradation and support bioaccumulation. Selenium, identified as essential trace nutrient metal for biological organism sustainability, is a non-metal element unique by having five different oxidation states, has attracted attention due to its excessive release through industrial activities. The main contributors to its release to the environment were reported to be petroleum refineries, phosphate mines, thermoelectric plants, solar batteries, semiconductors, agricultural drainage and sewage sludge [1, 2]. It is present as one of the volatile component in coal. Two common forms in which selenium is present in the natural soil environment are selenite (SeO_3^{2-}) and selenate (SeO_4^{2-}) even though elemental selenium and selenide are existing [3].

Irrigational discharge of selenium has been reported to discharge 75 to 1400 ppb of selenium into the soil ecosystem [4]. Nutritional requirement of selenium for the biological organisms was found to be 40 $\mu\text{g/g}$ and the threshold limit was reported as 165 ppb above which it could bring lethal effects [1, 4]. The aquatic tolerance level of selenium during indefinite exposure was listed as 5.0 $\mu\text{g/L}$ and updated recently [5]. Studies on removal of selenium using precipitation by zero valent iron [6], ferric hydroxide co-precipitation [7], photocatalytic reduction using UV [8], plant based biosorbent [3] and biological methods using bacterial reduction [9] have been reported. The common challenges associated with these methods are lower inlet load of selenium waste water, its multiple oxidation states and selectivity of the method of treatment. This often results in leading to poor removal efficiency, increased operating time and a large equipment size. Nanocomposites have emerged as an alternative for the removal of contaminants due to their target orientation and tailor made surface configuration and are applied in sensing, separation, fuel cells and catalytic processes [10, 11]. Even though many sol-gel based derivatization methods are available, there is always a need to identify a novel method with high selectivity.

Nano hydroxy apatite has been applied to remove fluoride either alone or in combination with chitosan [12]. The results of these abovementioned studies confirmed the need of composite, which is more biologically compatible as the hybrid sorbents were found to be more effective than pure hydroxy apatite. In this research study, a breakthrough attempt was made by incorporating a naturally available tree based sorbent into the hydroxy apatite matrix through wet chemical precipitation method. The date palm tree bark powder was synthesized and utilized as a biomaterial component in the nanocomposite. The experiments to validate the effect of process parameters were conducted along with equilibrium and kinetic modelling. The nanocomposite surface structure was characterized using FTIR and SEM techniques.

2. Methods

2.1. Synthesis of nanocomposite

Phoenix *dactylifera*, commonly known as date palm, is a monocot belonging to the family Arecaceae. Due to its excessive presence and easy availability in Oman, this tree was identified as a source of biomass component in the novel nanocomposite sorbent synthesized in this study. The processing of the tree barks to synthesize the protonated biomass powder was explained in a previous study [13]. The surface area of the protonated *Phoenix dactylifera* biomass was determined and reported earlier.

The nano hydroxy apatite was synthesized using wet chemical precipitation method with the Ca/P ratio of 1.67 using calcium nitrate ($\text{Ca}(\text{NO}_3)_2$), and ammonium di hydrogen phosphate ($\text{NH}_4\text{H}_2\text{PO}_4$). The aqueous solution of ammonium di hydrogen phosphate was added to the mixture of calcium nitrate and PDB. A milky and fairly gelatinous precipitate obtained was rinsed with water and dried at 90 °C. A three stage calcination was carried out at 400 °C, 600 °C and 800 °C for 1, 2 and 4h respectively. The calcined powder termed as agro based nanocomposite (ABNC).

2.2. Metal solution

Selenium solutions of desired concentrations have been prepared by dissolving calculated quantity of Selenium dioxide (SeO_2), supplied by Merck, Germany. Stock solution containing 1000 ppm was prepared by dissolving 1.434 g of selenium dioxide in a 10% HCl (v/v) and diluted using double distilled water [1]. All other chemicals used in this study were AR Grade supplied by Sigma, USA.

2.3. Selenium removal experiments

Selenium removal experiments were conducted in an environmental shaker in order to identify the influence of process parameters namely pH, Selenium concentration, nanocomposite dose, speed and temperature. The influence of pH was studied in the range of 3.0-11.0 at a fixed Selenium concentration of 100 mg L⁻¹, sorbent dosage of 2.0 g L⁻¹ and agitation speed of 360 rpm. In the second set of experiments, the effect of different metal loadings represented in terms of initial selenium concentration was studied in the range of 50-200 mg L⁻¹ at optimal conditions of pH. Nanocomposite dosage was varied in the range of 0.5-6.0 g L⁻¹ at a fixed selenium concentration of 100 mg L⁻¹ and agitation speed of 360 rpm. The impact of co-existing chloride anion was verified by adding NaCl in the range of 0-10 g L⁻¹. All the experiments were conducted

at a controlled conditions of optimal pH, 100 mgL⁻¹ selenium concentration, shaking speed of 360 rpm and temperature of 35°C unless or otherwise specified.

2.4. Equilibrium studies

Equilibrium experiments were carried to determine the maximum removal potential of the nanocomposite under equilibrium conditions. The popularly used isotherm models, namely Langmuir and Freundlich models (Eqs. (1) and (2) respectively) were used to model the equilibrium data.

Langmuir isotherm is based on the assumptions: presence of monolayer sorption of sorbate on the sorbent surface and uniform energy of adsorption [14]. Contrarily, Freundlich isotherm represents the multilayer adsorption with molecular interaction. The linearized forms of the isotherms are given by:

$$\frac{c_e}{q_e} = \frac{c_e}{q_{max}} + \frac{1}{q_{max} K_L} \quad (1)$$

$$\ln q_e = \ln K_F + \frac{1}{n} \ln c_e \quad (2)$$

2.5. Metal analysis

The metal solutions before and after contact with the nanocomposite were filtered using 0.45 µm membrane filters and the filtrates were collected and analyzed for metal concentration using atomic absorption spectrophotometer (Perkin Elmer, USA). The removal efficiency percentage (RE %) of selenium was estimated using Eq. (3).

$$RE\% = \frac{(C_0 - C_e)}{C_0} \times 100 \quad (3)$$

The amount of metal adsorbed per unit mass of nanocomposite sorbent (or selenium uptake) was calculated using the Eq. (4).

$$q_e = \frac{V(C_0 - C_e)}{w} \quad (4)$$

2.6. Nanocomposite characterization

Nanocomposite material synthesized was analyzed for its surface properties and microstructure. The surface functional groups were identified using KBr pellets method performed using FTIR spectrophotometer (Perkin Elmer, USA) in the spectral range 400-4000 cm⁻¹. Scanning electron microscope (JEOL, Japan) with an accelerating voltage of 20 kV at high vacuum mode was employed to study the microstructure.

3. Results and discussion

3.1. Effect of pH

The selective removal of an ionic contaminant from a solution medium is largely dependent on its solubility, speciation properties and complex forming ability. pH is reported to be a vital factor contributing to the conditions favorable for selective metal removal by the nanocomposite adsorbent. To determine the effect of pH on

the sorption of Selenium by ABNC, experiments were conducted in the range of 3.0-11.0 with 100 mg L⁻¹ selenium concentration at an equilibrium time of 45 min.

Two regions were observed in the metal uptake curves and shown in Fig. 1. The maximum selenium uptake of 59.08 was observed at pH 3.0 and the values were found to be more or less stable till pH 5.0. When pH > 5.0, a sharp decrease in selenium uptake was noticed and the results were low in the entire pH range of 6.0 – 11.0. Better removal in the acidic pH range 3.0-5.0 was attributed to the zeta potential of the nanocomposite material. The point of zero charge was identified and the value of pH_{zpc} was identified as 4.90. When the solution pH is greater than pH_{zpc}, the surface of ABNC will be negatively charged. Selenium existing as selenite (SeO₃²⁻) and bi selenite (HSeO₃⁻) in the aqueous solution [2] will be repelled in the pH range of 5.0 -11.0 due to the abovementioned reason. Removal of selenium using nanoFe adsorbent reported similar changes in uptake with respect to acidic pH [4]. Removal efficiency consistent with the zeta potential values proved the vital role of surface potential floccs [15]. The optimal pH value was identified as 5.0 and used in all experiments conducted subsequently.

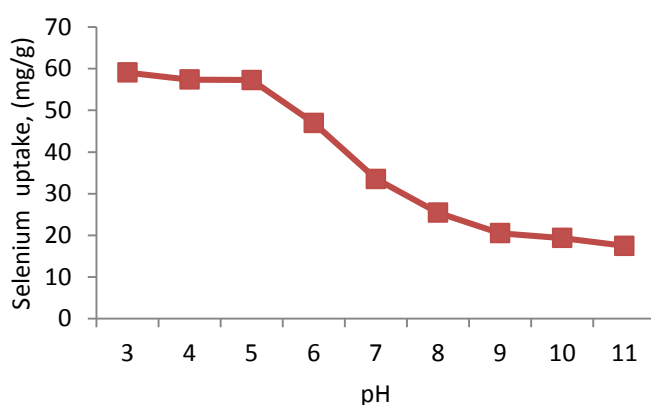


Fig. 1. Effect of initial pH on the uptake of selenium by ABNC.

3.2. Effect of contact time and initial metal concentration

Selenium initial concentration, a representative parameter of initial metal loading, was chosen in the range of 50-200 mg L⁻¹ in the second set of experiments and the results were presented in Fig. 2. The equilibrium selenium uptakes increased from 32.66 to 89.86 mg g⁻¹ when the initial selenium concentration increased from 50 to 200 mg/L. The increase in uptake values was attributed to higher ratio of sorbate ions to surface active sites at higher concentrations. The metal concentration acts as a driving force for mass transfer and increases the rate of diffusion and sorption. This driving force was reported to overcome the mass transfer resistance between the metal solution and sorbent surface [1]. The uptake curves showed two distinct zones, a primary rapid uptake zone and secondary stable zone. The optimal equilibrium time was identified as 45 minutes and used in all parametric experiments. Metal removal studies on selenium using nanoFe sorbent [4] and chitosan clay composite [16] presented similar results on the relationship between metal concentration and uptakes.

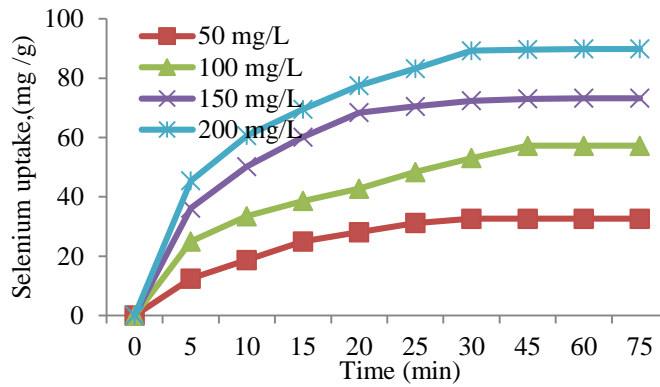


Fig. 2. Effect of contact time and initial selenium concentration on uptake by ANBC.

3.3. Effect of nanocomposite dose

The removal of selenium as a function of nanocomposite quantity was studied by varying the dosage of the sorbent added. From Fig. 3, it was inferred that the removal efficiency increased with dose and the increased availability of surface active sites was reported as the reason in many related studies [13, 16]. At higher nanocomposite dosage, the ratio between the unoccupied sites and free metal ions was higher. Increased availability of free sites always favored higher sorption of the selenium ions. However, the dependence of selenium uptake on nanocomposite dosage was found to be inverse with decreased uptakes observed at higher nanocomposite dosages. Superficial sorption and split in flux are reported to be the contribution factors for this negative impact on selenium uptake. The following empirical Eqs. 5 and 6 represent the relationship of selenium removal efficiency ($R^2 = 0.984$) and uptake ($R^2 = 0.937$) with nanocomposite dosage.

$$\text{Selenium uptake} = 202.3 (e^{-0.259 \cdot w}) \tag{5}$$

$$\text{Selenium removal efficiency} = 30.571 \ln(w) + 43.477 \tag{6}$$

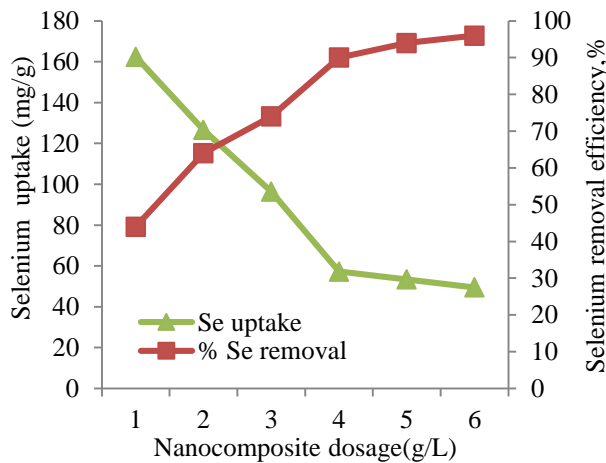


Fig. 3. Effect of nanocomposite dosage on the selenium removal efficiency and uptake.

3.4. Effect of salinity

Selenium, a naturally occurring metal in ground water, is expected to be accompanied by sodium chloride in the coastal areas. In order to determine the effect of salinity, experiments were conducted by adding sodium chloride as the competitor compound in the concentration range of 0-10 g L⁻¹. The blank experiment conducted without any addition of NaCl yielded 57.26 mg g⁻¹ and the metal uptake decreased with increase in NaCl concentration, as shown in Fig. 4. The selenium uptake decreased from 49 to 20.4 is mg g⁻¹ when the NaCl concentration was increased from 2 to 10 g L⁻¹, as shown in Fig. 4. Competition between selenium ions in dissolved form and chloride ions was identified as the reason for this inhibitive effect. The ratio of available surface active sites to total ions in solution increased due to the addition of NaCl. Presence of competitor ions in poly ionic solution always contributed to reduced uptake of target ions [17].

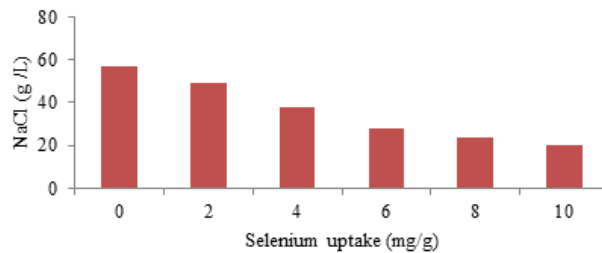


Fig. 4. Effect of salinity on the uptake of selenium.

3.5. Effect of agitation speed

Nanocomposite substances with increased surface active sites require proper contact with the sorbate ions in order to ensure better mass transfer. Agitation speed is an operating parameter that contributes to the mixing phenomenon in any separation process. In this set of experiments, the agitation speed was varied in the range of 120-600 rpm and the uptakes were recorded. The selenium uptake value reached its maximum at a speed of 360 rpm and decreased further at the speeds of 480 and 600 rpm and shown in Fig. 5. Reduction in the boundary layer thickness and enhanced homogeneity were found to be make positive contributions to selenium uptake. Excessive shear force at higher speeds could result in desorption of the metal ions from the surface active sites. Based on the results observed, the operational speed was fixed as 360 rpm.

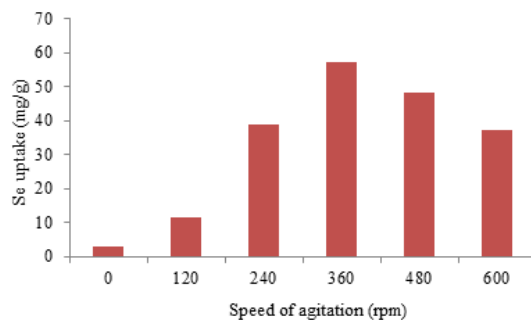


Fig. 5. Effect of speed of agitation on the uptake of selenium.

3.6. Equilibrium studies

To identify the appropriate isotherm model to represent the experimental data precisely, Langmuir and Freundlich isotherms were fitted and the goodness of fit was verified through linear regression. Fig. 6 represent the linearized form of Langmuir model and the model constants (q_{max} and K_L) were evaluated. Freundlich isotherm was fitted as shown in Fig. 7 whose slope and intercept gave the model constants (n and K_F). The constants were tabulated in Table 1. Langmuir isotherm was found to be more applicable for this research study with comparatively higher values of R^2 (> 0.985). The Langmuir constant (q_{max}) increased with increase in temperature and the values ranged between 95 and 114 mg g^{-1} . This result confirmed the presence of homogeneous monolayer sorption and the suitability was proved by the values of $R_L (= 1/(1 + K_L C_0))$ ranging between 0.05 and 0.07. The maximum uptake capacities obtained in this research were better than the values reported in removal of selenium using *E. camaldulensis* [4] and chitosan-clay composite [16].

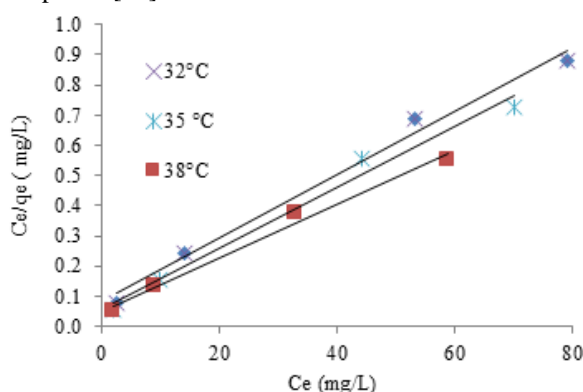


Fig. 6. Langmuir isotherm model for removal of selenium.

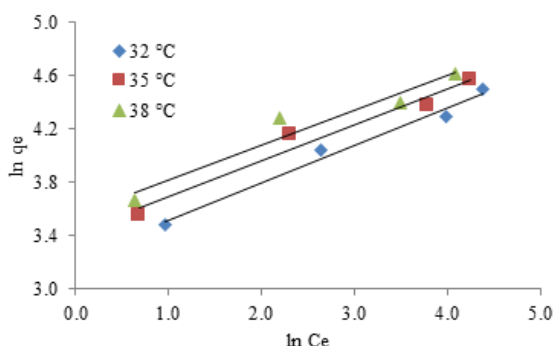


Fig. 7. Freundlich isotherm model for removal of selenium.

3.7. Modeling of sorption data

Kinetic experiments are aimed to verify the relationship between rate of sorption and initial sorbate concentration. The kinetic experiments were conducted with initial selenium concentration in the range of 50-200 mg L^{-1} under optimized process conditions pH 5.0, nanocomposite dose 4.0 g L^{-1} , shaking speed 360 rpm

and temperature 32°C. In this research, the pseudo-second-order equation [17, 18] represented by Eq.7 was applied to the experimental data to analyze the adsorption kinetics of Selenium ions. Modified Ritchie kinetic model shown in Eq. 8 is based on the assumption that the rate of adsorption depends solely on the fraction of sites unoccupied at any time t and was applied to the experimental data and evaluated [19, 20].

$$\frac{t}{q_t} = \frac{1}{k_2 q_e^2} + \frac{1}{q_e} t \quad (7)$$

$$\frac{t}{q_t} = \frac{1}{k_R q_e t} + \frac{1}{q_e} \quad (8)$$

Figures 8 and 9 represent the pseudo second order and modified Ritchie kinetic models respectively. In comparison, the pseudo second order model showed better suitability than the other model with higher values of R^2 (> 0.992). The pseudo-second order model constant decreased from 2.23 to 1.15 g (mg min) $^{-1}$ when temperature increased from 32 to 38°C. This observation confirmed the endothermic nature of selenium sorption onto the nanocomposite. Modified Ritchie kinetic model constants were evaluated and the modified Ritchie model rate constant decreased with increase in initial selenium concentration and presented in Table 2.

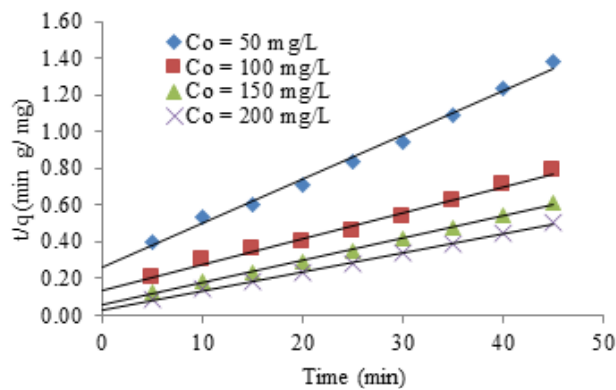


Fig. 8. Pseudo-second-order kinetic plots for the sorption of Se at 32°C.

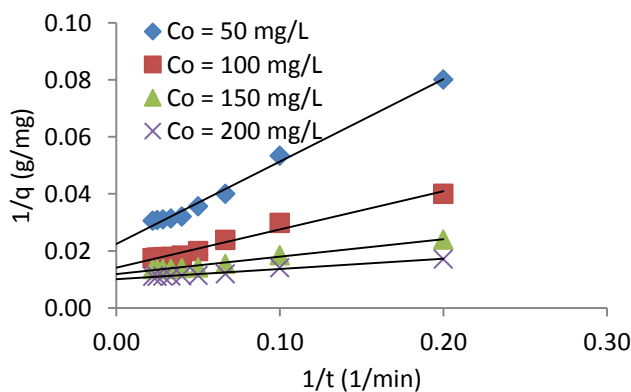


Fig. 9. Modified Ritchie kinetic plots for the sorption of Se at 32°C.

Table 1. Isotherm constants for removal of selenium.

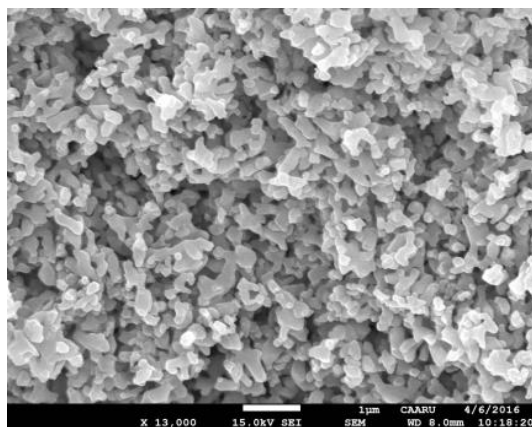
<i>T</i> °C	Langmuir constants		Freundlich constants			
	q_{max} (mg/g)	K_L (L/mg)	R^2	1/n	K_F (L/g)	R^2
32	95.24	0.129	0.989	0.281	3.242	0.983
35	100.00	0.176	0.986	0.269	3.421	0.965
38	113.64	0.180	0.989	0.261	3.560	0.938

Table 2. Kinetic constants for the removal of selenium by ABNC at 32°C.

Pseudo-second order model				Modified Ritchie kinetic model		
C_0 (mg/L)	q_e (mg/g)	$k_2 \times 10^3$ (g /mg min)	R^2	q_e (mg/g)	$k_R \times 10^2$ (min)	R^2
50	41.67	2.23	0.992	44.64	7.74	0.990
100	70.92	1.50	0.992	70.92	1.41	0.980
150	81.30	1.35	0.997	84.75	1.18	0.987
200	97.09	1.15	0.996	100.00	1.00	0.976

3.8. SEM imaging

The microstructure of the sorbent was shown in Fig. 10 and microscopy imaging confirms the presence of active sites in the matrix of nanocomposite. Nanocomposite adsorbent showed good microcrystalline cross section and proved very efficient in the removal of selenium from aqueous solution. The higher uptakes at 100 mg L⁻¹ selenium concentration proved the capacity of the sorbent surface.

**Fig. 10. SEM imaging of nanocomposite microstructure.**

3.9. FTIR studies

The nanocomposite sorbent surface was analyzed using FTIR and the active functional groups. The bonds related to the functional groups were identified as C-O stretch, C-N stretch and O-H bend based on characteristic IR absorption ranges.

4. Conclusion

In this research study, a nanocomposite adsorbent was synthesized using wet chemical precipitation method using hydroxy apatite and date palm tree powder and feasibility of its application for selenium removal was studied. pH was found to influence the removal uptake and the optimal pH was identified as 5.0. The nanocomposite dose was optimized and found to have direct proportionality with metal removal efficiency.

The nanocomposite sorbent achieved a selenium uptake of 57.26 mg g⁻¹ with 100 mg L⁻¹ selenium concentration under optimal conditions. From equilibrium experiments, Langmuir model fitted the data well and the isotherm constants were evaluated to be $q_{max} = 95.238$ mg g⁻¹ and $K_L = 0.129$ L mg⁻¹. The kinetic modeling was represented well by pseudo second order model, which proved better than modified Ritchie model. Higher temperatures resulted in lower values of rate constant and the sorption process was found to be favorable under endothermic environment. Nanocomposite was characterized using FTIR and SEM imaging.

References

1. Khakpour, H.; Younesi H.; and Mohammadhosseini, M. (2013). Two stage biosorption of selenium from aqueous solution using dried biomass of the baker's yeast *Saccharomyces cerevisiae*. *Journal of Environmental Chemical Engineering*, 2(1), 532-542.
2. Santos, S.; Ungureanu, G.; Boaventura, R.; and Botelho C. (2015). Selenium contaminated waters: An overview of analytical methods, treatment options and recent advances in sorption methods. *Science of the Total Environment*, 521-522, 246-260.
3. Rajamohan, N.; and Rajasimman M. (2015). Biosorption of selenium using activated plant based sorbent - Effect of variables, isotherm and kinetic modelling. *Biocatalysis and Agricultural Biotechnology*, 4(4), 795-800.
4. Zelmanov, G.; and Semiat, R. (2013). Selenium removal from water and its recovery using iron (Fe³⁺) oxide/hydroxide-based nanoparticles sol (NanoFe) as an adsorbent. *Separation and Purification Technology*, 103, 167-172.
5. APHA (2014). *Standard methods for the examination of water and wastewater*, (22nd ed.). Washington DC: American Public Health Association/American Water Works Association/Water Environment Federation.
6. Zhang, Y.; Amrhein, C.; and Frankenberger Jr., W.T. (2005). Effect of arsenate and molybdate on removal of selenate from an aqueous solution by zero-valent iron. *Science of the Total Environment*, 350(1-3), 1-11.
7. Sharrad, M.O.M.; Liu, H.; and Fan, M. (2012). Evaluation of FeOOH performance on selenium reduction. *Separation and Purification Technology*, 84, 29-34.
8. Nguyen, V.N.H.; Beydoun, D.; and Amal, R. (2005). Photo-catalytic reduction of selenite and selenate using TiO₂ photo-catalyst. *Journal of Photochemistry and Photobiology A: Chemistry*. 171(2), 113-120.

9. Zhang, Y.; Okeke, B.C.; and Frankenberger Jr., W.T. (2008) Bacterial reduction of selenate to elemental selenium utilizing molasses as a carbon source. *Bioresource Technology*, 99(5), 1267-1273.
10. Arshadi, M. (2015). Manganese chloride nanoparticles: A practical adsorbent for the sequestration of Hg (II) ions from aqueous solution. *Chemical Engineering Journal*, 259, 170-182.
11. Sundaram, C.S.; Viswanathan, N.; and Meenakshi, S. (2008). Defluoridation chemistry of synthetic hydroxyapatite at nano scale: equilibrium and kinetic studies. *Journal of Hazardous Materials*, 155(1-2), 206-215.
12. Rajamohan, N.; Dilipkumar, M.; and Rajasimman M. (2014). Parametric and kinetic studies on biosorption of mercury using modified Phoenix dactylifera biomass. *Journal of the Taiwan Institute of Chemical Engineers*, 45(5), 2622-2627
13. Langmuir, I. (1916). The constitution and fundamental properties of solid and liquids. Part 1. Solid. *Journal of the American Chemical Society*, 38(11), 2221-2295
14. Hu, C.; Chen, Q.; Chen, G.; and Qu, J. (2015). Removal of Se (IV) and Se (VI) from drinking water by coagulation. *Separation and Purification Technology*, 142, 65-70.
15. Bleiman, N.; and Mishael, Y.G. (2010). Selenium removal from drinking water by adsorption to chitosan-clay composites and oxides: Batch and column tests. *Journal of Hazardous Materials*, 183(1-3), 590-595.
16. Fu, F.; and Wang Q. (2011). Removal of heavy metal ions from wastewaters. *Journal of Environment Management*, 92(3), 407-418.
17. Ho, Y.S.; and McKay G. (1999). Pseudo-second order model for sorption processes. *Process Biochemistry*, 34(5), 451-465.
18. Ho, Y.S. (2006). Second-order kinetic model for the sorption of cadmium onto tree fern: A comparison of linear and non-linear methods. *Water Research*, 40(1), 119-125.
19. Liu, J.; Wu L.; and Chen X. (2015). Kinetic model investigation on lead (II) adsorption using silica-based hybrid membranes. *Desalination and Water Treatment*. 54(8), 2307-2313.
20. Holmes, A.B; and Gu, F.X. (2016). Emerging nanomaterials for the application of selenium removal for wastewater treatment. *Environmental Science: Nano*, 5(3), 982-996.